INHOMOGENEOUS STELLAR MODELS. III. MODELS WITH PARTIALLY DEGENERATE ISOTHERMAL CORES*

M. SCHWARZSCHILD, I. RABINOWITZ, AND R. HÄRM
Princeton University Observatory
Received March 30, 1953

ABSTRACT

A search was made for conditions under which models with partially degenerate isothermal cores could give radii as large as those of red giants. Special conditions were found for which detailed computations gave, indeed, models fitting well the red giants in radius and luminosity. But it has not been investigated whether the special conditions are likely to be realized in the evolution of a star.

I. INTRODUCTION

If a star during the early stages of its evolution possesses no appreciable mixing currents in its interior, the central portion of this star will in time burn out of fuel, and an exhausted, isothermal core will form. Stellar models with isothermal nondegenerate cores were investigated by Schönberg and Chandrasekhar;[1] they found that these models were fairly similar to the Cowling model and that, hence, stars built according to these models should fall reasonably close to the main sequence in the Hertzsprung-Russell diagram. Following this investigation, Gamow and Keller[2] made approximate computations regarding models with isothermal cores in a partially degenerate state; these computations appear to indicate that under certain circumstances such models could give very large radii—large enough to fit the red giants. Subsequently M. H. Harrison[3] accurately computed an array of models with partially degenerate isothermal cores; none of these models showed large radii. This result, however, is not certain to be general, since the cases considered by Mrs. Harrison were selected according to certain considerations regarding stellar evolution.

At present the internal evolution of a star still seems quite uncertain; in particular, the existence, extent, and strength of mixing currents as a function of time during the evolution are still fairly unknown. It therefore appeared useful to extend the earlier accurate computations without restrictions following from evolutionary considerations. A first such extension was carried out by M. Hayashi,[4] who, however, restricted himself to a particular composition for the envelopes. A more general extension is presented in this paper.

It is the purpose of the present investigation to check by accurate computations under which circumstances models with partially degenerate isothermal cores will give radii as large as those of red giants.

II. APPROXIMATIONS AND BASIC EQUATIONS

The models here to be considered consist of two zones: (1) a partially degenerate isothermal core with a composition of 98 per cent helium and 2 per cent heavy elements,

* This research was supported in part by funds of the Eugene Higgins Trust allocated to Princeton University and in part by contract with the Office of Naval Research.

[1] *Ap. J.*, **96**, 161, 1942.

[2] *Rev. Mod. Phys.*, **17**, 125, 1945.

[3] *Ap. J.*, **103**, 193, 1946.

[4] *Phys. Rev.*, **75**, 1619, 1949.

i.e., without nuclear fuel (accordingly, the molecular weight in the core is $\mu_i = 1.342$, the same for all models); (2) a radiative envelope of composition different from the core (whenever the envelope is given the same molecular weight as the core, this is meant as a limit for a small hydrogen content in the envelope but is not meant to represent an exhausted envelope).

In order to facilitate the integration of the equations and the fitting of the models, the following simplifying approximations are made:

a) The energy generation takes place in an infinitesimally thin shell at the interface between core and envelope.

b) The temperature of this shell—and hence in the entire core—is 30,000,000°, so that the carbon cycle can proceed at the required rate.

c) The composition changes discontinuously at the interface between the hydrogen-containing envelope and the burned-out core.

d) The absorption coefficient in the radiative envelope is given by Kramers' law as

$$\kappa = \kappa_0 \rho T^{3-3.5} \qquad \text{with} \qquad \kappa_0 = 2 \times 10^{25} Z(1+X) , \tag{1}$$

corresponding to a guillotine factor of $(t/\bar{g}) = 2$.

e) Radiation pressure is negligible.

f) The mean molecular weight in the core, μ_i, is computed to correspond to the total number of particles, not of the electrons alone. Thus the correct equation of state is used in the outer, nondegenerate portion of the core, while in the inner portion the degenerate pressure is exaggerated by a factor of 1.5 for helium—an error presumably tolerable for the present purpose.

The following definitions and equations form the basis for the computations.

Subscripts:

i for the core (interior),
e for the envelope,
1 for the interface,
c for the center (except for the central degeneracy, which is ψ_0).

Dimensionless variables p, t, q, and x for the envelope:

$$P = p \frac{GM^2}{4\pi R^4}, \qquad T = t \frac{\mu_e H}{k} \frac{GM}{R}, \qquad M_r = qM , \qquad r = xR . \tag{2}$$

Differential equations for the envelope:

$$\frac{dp}{dx} = -\frac{pq}{tx^2}, \qquad \frac{dq}{dx} = \frac{px^2}{t}, \qquad \frac{dt}{dx} = -C \frac{p^2}{x^2 t^{8.5}}, \tag{3}$$

with

$$C = \frac{3}{4ac} \kappa_0 \left(\frac{k}{\mu_e HG}\right)^{7.5} \left(\frac{1}{4\pi}\right)^3 \frac{LR^{0.5}}{M^{5.5}}. \tag{4}$$

Homology invariants in envelope:

$$U = \frac{px^3}{tq}, \qquad V = \frac{q}{tx}. \tag{5}$$

Dimensionless variables ξ and ψ for the core:

$$r=\frac{h^{3/2}}{4\pi\mu_i H}(2mkT)^{-1/4}(2mG)^{-1/2}\xi\,, \tag{6}$$

$$\rho=\frac{4\pi}{h^3}(2mkT)^{3/2}\mu_i HF_{1/2}(\psi)\,, \tag{7}$$

$$P=\frac{8\pi}{3h^3}(2mkT)^{3/2}kTF_{3/2}(\psi)\,, \tag{8}$$

where the Fermi-Dirac integral is defined by

$$F_\nu(\psi)\int_0^\infty\frac{u^\nu}{e^{u-\psi}+1}du\,. \tag{9}$$

Differential equation for core:

$$\frac{1}{\xi^2}\frac{d}{a\xi}\left(\xi^2\frac{d\psi}{a\xi}\right)=-F_{1/2}(\psi)\,. \tag{10}$$

Homology invariants for core:

$$U=\frac{F_{1/2}(\psi)\,\xi^3}{\left(-\xi^2\frac{d\psi}{d\xi}\right)},\qquad V=\frac{F_{1/2}(\psi)}{F_{3/2}(\psi)}\cdot\frac{3}{2\xi}\cdot\left(-\xi^2\frac{d\psi}{d\xi}\right). \tag{11}$$

Fitting conditions at the interface between core and envelope, where the jump in molecular weight occurs:

$$\frac{U_{1i}}{U_{1e}}=\frac{V_{1i}}{V_{1e}}=l\qquad\text{with}\qquad l=\frac{\mu_i}{\mu_e}. \tag{12}$$

For the envelope, ten particular solutions of equations (3) (corresponding to ten values of the parameter C), with the boundary conditions that $p=t=0$ and $q=1$ at $x=1$, were obtained by numerical integration.[5] Five of these solutions are shown in Figure 1 in terms of the U–V plane.

For the core, G. W. Wares[6] has obtained eight particular solutions of equation (10) (corresponding to eight values of ψ_0, the degeneracy at the center). Five of these solutions are shown in Figure 1 in terms of the U–V plane.

III. PRELIMINARY ORIENTATION IN THE U–V PLANE

The family of models here to be considered has three free parameters. In dimensionless terms, one may use for these parameters ψ_0 (which fixes the particular core solution to be used); ξ_1 (which fixes the end-point on the core solution, i.e., U_{1i} and V_{1i}, at which the jump to the envelope solution should occur); and l (which, according to eq. [12], gives the length of the jump in the U–V plane and hence the starting point U_{1e} and V_{1e}, from which the envelope solution should be followed out to the surface). In physical terms, the three free parameters are the total mass of the star, M; the fraction of the total mass in the exhausted core, q_1; and the ratio of the molecular weights in core and envelope, l. The explicit occurrence of M as an independent parameter here is caused by

[5] To be published in a forthcoming *Princeton U. Obs. Contr.*

[6] *Ap. J.*, **100**, 158, 1944; also "Partially Degenerate Stellar Models" (dissertation, University of Chicago, 1940).

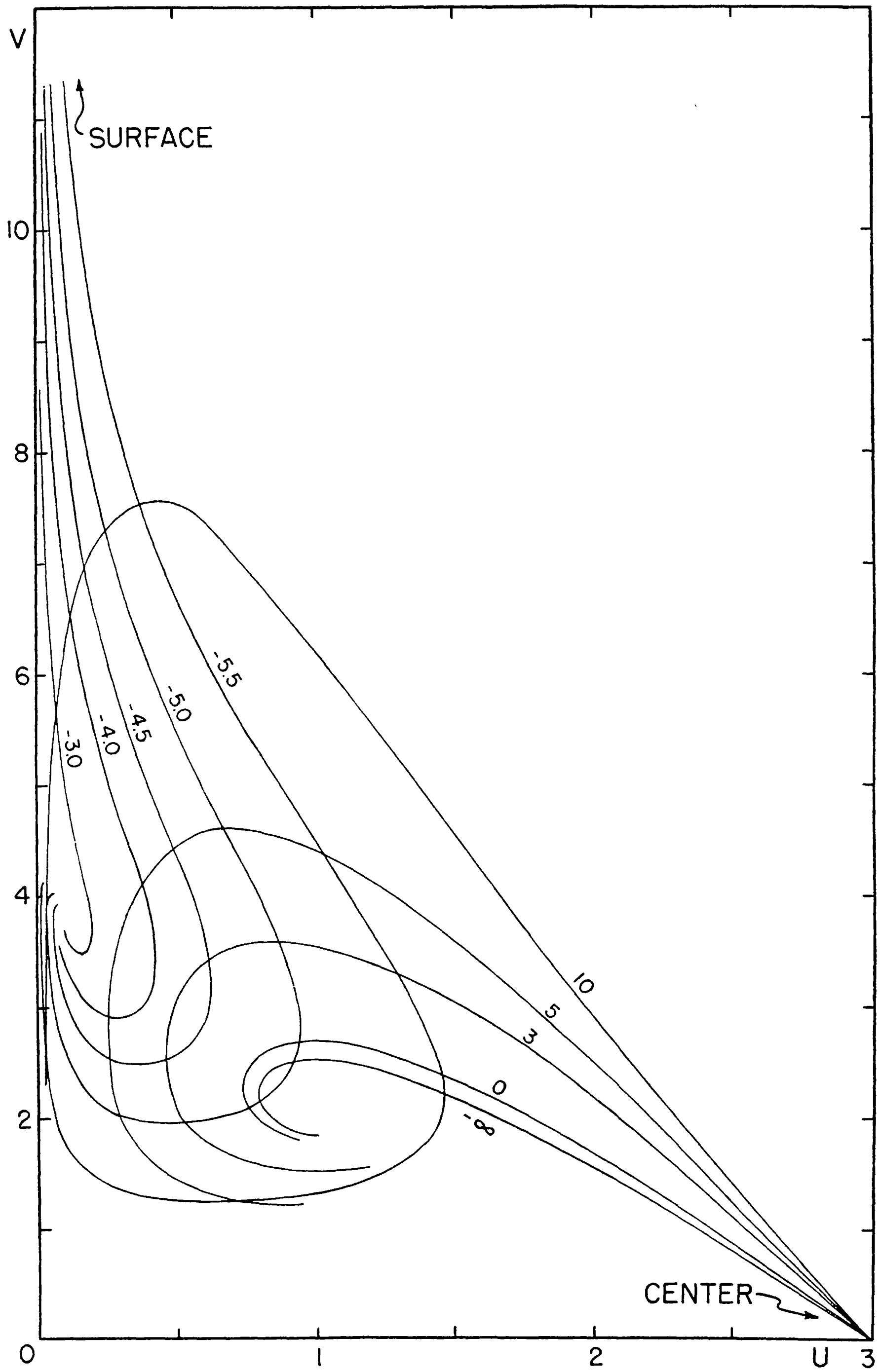

FIG. 1.—Solutions for the cores and envelopes in the U−V plane. The envelope solutions are labeled by values of log C, the core solutions by ψ_0. The solution labeled $-\infty$ is the nondegenerate isothermal core.

the complicated equation of state here used. It introduces a computational complication not found in such nondegenerate models as those discussed in the preceding papers of this series, where the mass could be transformed away by a homology transformation.

Since it does not seem practicable at present to cover the three-parameter family of models completely by individual numerical examples, it appears necessary, first, to find out in which part of the U–V plane the physically interesting cases are to be found. Such a survey was carried out as follows.

If for this survey $l = 1$ is used, any model can be represented in the U–V plane by the point U_1, V_1, which characterizes the interface between core and envelope. The representative points of all the models which have the same value of the mass will form a curve in the U–V plane. Such curves of constant mass may be derived as follows: The value of the density at the interface can be expressed in terms of p_1 and t_1 by the first two equations (2). The same density value can also be expressed in terms of $F_{1/2}(\psi_1)$ by equation (7). Setting the two expressions equal, one obtains an equation which, besides dimensionless variables, involves M and R. Eliminating R with the help of the second equation (2), one obtains for M

$$M = \frac{p_1^{1/2}}{t_1^2} F_{1/2}^{-1/2}(\psi_1) \left(\frac{h^2 k T_1}{2G^2 m}\right)^{3/4} \left(\frac{1}{2\pi^{1/2}\mu_e H}\right)^2 . \tag{13}$$

With $\mu_e = 1.342$ and $T_1 = 30{,}000{,}000°$, the two right-hand factors in this equation are known constants. Regarding the first factor, p_1 and t_1 can be interpolated from the envelope solutions for any point in the U–V plane. Similarly for the second factor, $F_{1/2}(\psi_1)$ can be interpolated from the core solutions. Therefore, M can be computed for any point in the U–V plane, and points of equal M can then be connected by curves. These curves of constant M are shown in Figure 2, *a*. The curve corresponding to 1.8 solar masses may be thought of as the center line of a strip containing all the models with masses of the right order for red giants.

Next, curves connecting all representative points corresponding to the same mass fraction in the exhausted core may be obtained. Since for any point in the U–V plane the value of q_1 is directly given by the value of q on that envelope solution which goes through the point in question, the curves of constant q_1 are the curves of constant q drawn across the envelope solutions. These curves are shown in Figure 2, *b*. The approximate parallelity of the curves of constant M and those of constant q_1 indicates that for a given mass a small change in q_1 can produce large changes in the model.

Finally, to be able to judge which of these models may have large radii to fit the red giants, the curves of t_1 are to be constructed, since, according to the second equation (2), a large value of t_1 corresponds to a large radius. The curves of constant t_1 are again identical with the curves of constant t drawn across the envelope-curves—which are also shown in Figure 2, *b*. This figure indicates that large t_1 values, and hence large radii, are to be found only rather far to the left in the U–V plane.

The curves of constant M in Figure 2, *a*, and the curves of constant t_1 in Figure 2, *b*, together delineate a narrow section in the U–V plane in which the representative points are to be found which give models of the proper masses and radii for red giants. The construction of models thus selected is described in the following section.

IV. CONSTRUCTION OF THE MODELS

Two methods of construction of models were used to get the models whose characteristics are given in Table 1. For models *j*, *k*, *l*, and *m* the procedure was as follows:

Using the U–V plane shown in Figure 1, we start on a given envelope-curve (thus fixing the value of C and hence the mass-luminosity relation) and choose an arbitrary value of x_1. Thus U_{1e} and V_{1e} are determined. Next, choosing a value of l, we jump radially outward from the origin, so as to satisfy condition (12), which fixes U_{1i} and V_{1i}. Finally, the appropriate core solution is found by interpolation at the point U_{1i}, V_{1i} between the available core solutions.

After the fitting is accomplished in the U–V plane, the mathematical characteristics of the models can be derived as follows: $\log p_1$, $\log t_1$, $\log q_1$, U_{1e}, and V_{1e} are read directly from the numerical integrations for the envelope in accordance with the C and x_1 values chosen. With the help of equation (12), U_{1i} and V_{1i} are obtained; ψ_0 is determined by the interpolation between the core integrations; and $F_{1/2}(\psi_0)$ and $F_{3/2}(\psi_0)$ are read from the available tables of the Fermi-Dirac integrals.[7] The value of $F_{1/2}(\psi_1)$ is found by

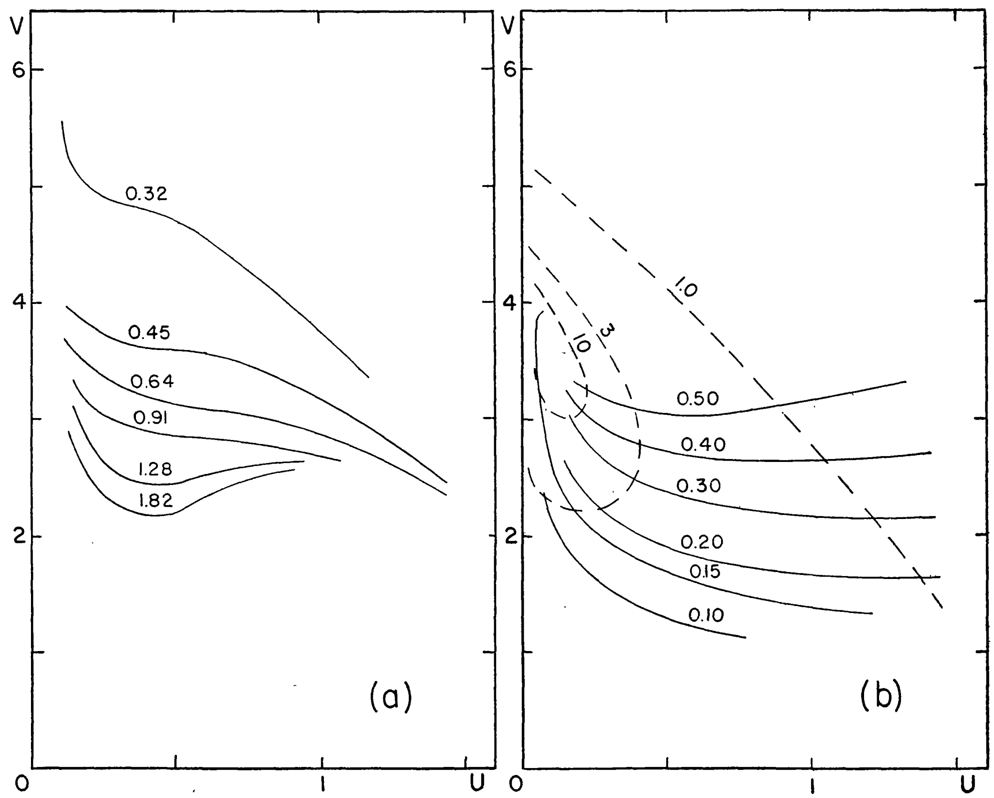

FIG. 2.—*a*, curves of constant mass for models with no jump in molecular weight. *b*, curves of constant q (*solid lines*) and of constant t (*dashed lines*), as determined from the envelope integrations.

interpolation between curves of constant $F_{1/2}(\psi_1)$ drawn across the core integrations in the U–V plane, and ψ_1 is determined from $F_{1/2}(\psi_1)$ by inverse interpolation in the above-mentioned tables.

The second method of fitting, which produced models *a*–*i*, was as follows: The models were assumed to have a core mass of 15 per cent. The curve $q_1 = 0.15$ was drawn by interpolation in the envelope-curves, and the jump-off point (U_{1e}, V_{1e}) was selected arbitrarily on it. Further, the point U_{1i}, V_{1i} was again obtained from equation (12). As before, it was necessary to interpolate between the core solutions in order to find ψ_0, ψ_1, $F_{1/2}(\psi_0)$, $F_{3/2}(\psi_0)$, and $F_{1/2}(\psi_1)$. However, since the jump-off point on the $q_1 = 0.15$ curve did not, in general, lie along one of the envelope-curves, it was here also necessary to interpolate between the envelope integrations to find $\log C$, x_1, p_1, and t_1.

[7] J. McDougall and E. C. Stoner, *Phil. Trans. R. Soc. London, A*, **237**, 67, 1938.

TABLE 1

MATHEMATICAL AND PHYSICAL CHARACTERISTICS OF MODELS

Characteristics	a	b	c	d	e	f	g	h	i	j	k	l	m
U_{1e}	+ 0.0608	+ 0.0608	+ 0.0608	+ 0.0471	+ 0.0471	+ 0.0471	+ 0.0512	+ 0.0512	+ 0.0512	+ 0.1304	+ 0.0986	+ 0.1304	+ 0.0986
V_{1e}	+ 3.223	+ 3.223	+ 3.223	+ 3.812	+ 3.812	+ 3.812	+ 3.936	+ 3.936	+ 3.936	+ 3.408	+ 3.704	+ 3.408	+ 3.704
U_{1i}	+ 0.0608	+ 0.0912	+ 0.1216	+ 0.0471	+ 0.0706	+ 0.0942	+ 0.0512	+ 0.0768	+ 0.1024	+ 0.1304	+ 0.0986	+ 0.2608	+ 0.1972
V_{1i}	+ 3.223	+ 4.834	+ 6.446	+ 3.812	+ 5.718	+ 7.624	+ 3.936	+ 5.904	+ 7.872	+ 3.408	+ 3.704	+ 6.816	+ 7.408
l	+ 1.0	+ 1.5	+ 2.0	+ 1.0	+ 1.5	+ 2.0	+ 1.0	+ 1.5	+ 2.0	+ 1.0	+ 1.0	+ 2.0	+ 2.0
log C	− 4.88	− 4.88	− 4.88	− 4.77	− 4.77	− 4.77	− 4.71	− 4.71	− 4.71	− 3.50	− 3.00	− 3.50	− 3.00
$1000x_1$	+ 4.9	+ 4.9	+ 4.9	+ 0.94	+ 0.94	+ 0.94	+ 0.32	+ 0.32	+ 0.32	+ 3.15	+ 0.282	+ 3.15	+ 0.282
log p_1	+ 5.84	+ 5.84	+ 5.84	+ 8.58	+ 8.58	+ 8.58	+10.78	+10.78	+10.78	+ 7.701	+11.729	+ 7.701	+11.729
log t_1	+ 0.98	+ 0.98	+ 0.98	+ 1.63	+ 1.63	+ 1.63	+ 2.12	+ 2.12	+ 2.12	+ 1.525	+ 2.533	+ 1.525	+ 2.533
q_1	+ 0.15	+ 0.15	+ 0.15	+ 0.15	+ 0.15	+ 0.15	+ 0.15	+ 0.15	+ 0.15	+ 0.360	+ 0.360	+ 0.360	+ 0.360
ψ_0	+ 8.70	+ 8.77	+ 9.83	+ 9.42	+10.15	+11.80	+ 9.35	+10.16	+12.25	+ 6.95	+ 7.90	+ 9.18	+10.50
log $F_{1/2}(\psi_0)$	+ 1.240	+ 1.245	+ 1.318	+ 1.291	+ 1.339	+ 1.436	+ 1.286	+ 1.339	+ 1.460	+ 1.098	+ 1.179	+ 1.275	+ 1.361
log $F_{3/2}(\psi_0)$	+ 1.985	+ 1.993	+ 2.110	+ 2.066	+ 2.143	+ 2.301	+ 2.059	+ 2.144	+ 2.340	+ 1.759	+ 1.887	+ 2.040	+ 2.179
ψ_1	− 5.25	− 3.70	− 2.54	− 5.04	− 3.52	− 2.48	− 4.85	− 3.40	− 2.04	− 4.12	− 4.21	− 1.35	− 1.52
log $F_{1/2}(\psi_1)$	− 2.333	− 1.663	− 1.167	− 2.242	− 1.585	− 1.130	− 2.160	− 1.534	− 0.957	− 1.844	− 1.883	− 0.675	− 0.744
X_e	0.0	+ 0.298	+ 0.596	0.0	+ 0.298	+ 0.596	0.0	+ 0.298	+ 0.596	0.0	0.0	+ 0.596	+ 0.596
μ_e	+ 1.342	+ 0.895	+ 0.671	+ 1.342	+ 0.895	+ 0.671	+ 1.342	+ 0.895	+ 0.671	+ 1.342	+ 1.342	+ 0.671	+ 0.671
log ρ_{1e}	+ 0.970	+ 1.46	+ 1.84	+ 1.07	+ 1.54	+ 1.87	+ 1.14	+ 1.59	+ 2.04	+ 1.46	+ 1.42	+ 2.33	+ 2.26
log ρ_c	+ 4.54	+ 4.55	+ 4.62	+ 4.59	+ 4.64	+ 4.74	+ 4.59	+ 4.64	+ 4.76	+ 4.40	+ 4.48	+ 4.58	+ 4.66
log P_c	+20.38	+20.39	+20.50	+20.46	+20.54	+20.69	+20.45	+20.54	+20.73	+20.15	+20.28	+20.43	+20.57
$M/M_\odot$	+ 1.9	+ 2.0	+ 2.0	+ 2.1	+ 2.2	+ 2.3	+ 2.5	+ 2.7	+ 2.5	+ 0.77	+ 0.80	+ 0.80	+ 0.86
$R/R_\odot$	+19	+13	+10	+91	+64	+51	+340	+250	+170	+27	+280	+14	+150
$L/L_\odot$	+14,000	+780	+87	+12,000	+680	+110	+19,000	+1,300	+92	+1,700	+2,100	+10	+15
log T_e	+ 4.15	+ 3.92	+ 3.74	+ 3.79	+ 3.56	+ 3.42	+ 3.56	+ 3.34	+ 3.13	+ 3.85	+ 3.36	+ 3.44	+ 2.96
M_{bol}	− 5.8	− 2.6	− 0.2	− 5.5	− 2.5	− 0.5	− 6.0	− 3.2	− 0.3	− 3.5	− 3.7	+ 2.1	+ 1.7

The remaining quantities in Table 1 relate to the physical characteristics of the models and were determined from the mathematical properties enumerated above as follows: Since we assume l and μ_i (l varying from model to model, μ_i the same for all models), we find μ_e from equation (12), and since we assume $Z_e = Z_i = 0.02$, we find X_e from μ_e. The central density and pressure, ρ_c and P_c, are obtained from equations (7) and (8). The mass is found from equation (13), and the radius from the second equation (2). The luminosity is derived from equation (4), and then the effective temperature and bolometric absolute magnitude follow at once. Finally, the density at the interface, ρ_{1e}, is obtained from the first two equations (2).

V. PHYSICAL CHARACTERISTICS OF MODELS

To judge how far the models here constructed are applicable to observed stars, the model stars have been plotted in a Hertzsprung-Russell diagram (Fig. 3) according to the

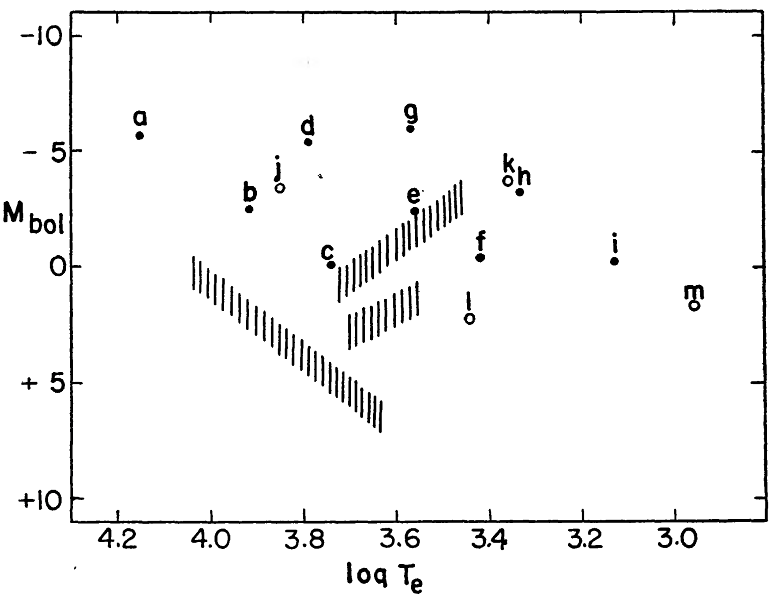

FIG. 3.—Hertzsprung-Russell diagram. The thirteen lettered symbols correspond to the models listed in Table 1. The dots represent cases in which the core contains 15 per cent of the mass (stellar masses from 1.9 to 2.7 solar masses), whereas the circles represent cases in which the core contains 36 per cent of the mass (stellar masses around 0.8 solar masses). The hatched regions indicate schematically the observed locations of the giants, subgiants, and main-sequence stars.

bolometric magnitudes and effective temperatures listed in Table 1. Figure 3 shows that the present models cover well the area occupied by the red giants. Hence the present detailed computations appear to substantiate the earlier tentative conclusions by Gamow and Keller[2] that models with partially degenerate isothermal cores may under certain circumstances have very large radii.

On the other hand, most of the models here considered—all but the four referring to relatively small stellar masses—have a rather small fraction of their mass in the isothermal core. Indeed, the mass of the core for all thirteen models lies between 28 and 40 per cent of a solar mass. Hence the masses of the isothermal cores—and even more the masses of the degenerate parts of the isothermal cores—lie well below the limit for a degenerate mass. This is in agreement with the general considerations pointed out by Chandrasekhar.[3]

After having compared the model stars with the observed red giants in terms of the

Hertzsprung-Russell diagram, i.e., in terms of luminosities and radii, it remains to compare the theoretical and real stars in terms of their masses, or rather their mass-luminosity relations. The large log C values listed in Table 1 (compared with log $C = -6.0$ for the Cowling model) show that the present models are, on the average, 20 times more luminous than main-sequence stars of the same mass or that their masses are, on the average, two times smaller than those of main-sequence stars of the same luminosity. In this regard the present models are similar to those discussed in the first paper of this series,[8] and correspondingly the discussion of the masses of red giants given there applies here too. Accordingly, one may conclude here again that the observational data on the masses of red giant stars are still insufficient either to corroborate or to contradict the mass-luminosity relation of the present models.

Even though there is no apparent discrepancy between the present models and red giants as far as luminosities, radii, and masses are concerned, the following consideration makes it seem somewhat unlikely that partially degenerate isothermal cores should be the main cause of the red giant phenomenon. The data represented in Figure 2 indicate that for a given stellar mass, M, and for a given jump in the molecular weight, l, the fraction of the mass contained in the exhausted core, q_1, must fall within very narrow limits if the star is to be comparable with observed red giants. For smaller values of q_1 the models will lie very close to the main sequence and thus not represent red giants. The cases of larger q_1 values have not been investigated here; it appears, however, rather likely that for larger q_1 values either no equilibrium configuration exists (for a given M and l), much as in the Schönberg-Chandrasekhar case of nondegenerate isothermal cores, or these cases show radii even larger than those of the observed red giants. In any case, the red giants can apparently be fitted only by models with partially degenerate isothermal cores if q_1—as a function of M and l—falls within fairly narrow limits, as has already been indicated by M. Hayashi. It does not appear too likely that such narrow conditions can actually be fulfilled by the entire red giant class of stars.

One may then conclude that the observable characteristics of red giants can be fitted with models with partially degenerate isothermal cores but that this fit can apparently be achieved only if the exhausted core fulfils rather narrow conditions. Hence it appears possible that partially degenerate cores are a contributing factor, but probably are not the main cause, for the large radii of red giants.

We wish to thank Dr. S. Chandrasekhar and Dr. G. W. Wares for their generously making available to us Dr. Wares's integrations for partially degenerate cores.

[8] J. B. Oke and M. Schwarzschild, *Ap. J.*, **116**, 317, 1952.